
Cross Modal Distillation for Supervision Transfer

Saurabh Gupta

Judy Hoffman

Jitendra Malik

UC Berkeley

{sgupta, jhoffman, malik}@eecs.berkeley.edu

Abstract

In this work we propose a technique that transfers supervision between images from different modalities. We use learned representations from a large labeled modality as a supervisory signal for training representations for a new unlabeled paired modality. Our method enables learning of rich representations for unlabeled modalities and can be used as a pre-training procedure for new modalities with limited labeled data. We show experimental results where we transfer supervision from labeled RGB images to unlabeled depth and optical flow images and demonstrate large improvements for both these cross modal supervision transfers.

1 Introduction

Current paradigms for recognition in computer vision involve learning a generic feature representation on a large dataset of labeled images, and then specializing or finetuning the learned generic feature representation for the specific task at hand. Successful examples of this paradigm include almost all state-of-the-art systems: object detection [12], semantic segmentation [28], object segmentation [17], and pose estimation [38], which start from generic features that are learned on the ImageNet dataset [6] using over a million labeled images and specialize them for each of the different tasks. Several different architectures for learning these generic feature representations have been proposed over the years [25, 35, 3], but all of these rely on the availability of a large dataset of labeled images to learn feature representations.

The question we ask in this work is, what is the analogue of this paradigm for images from modalities which do not have such large amounts of labeled data? There are a large number of image modalities beyond RGB images which are dominant in computer vision, for example depth images coming from a Microsoft Kinect, infra-red images from thermal sensors, aerial images from satellites and drones, LIDAR point clouds from laser scanners, or even images of intermediate representations output from current vision systems *e.g.* optical flow and stereo images. The number of labeled images from such modalities are at least a few orders of magnitude smaller than the RGB image datasets used for learning features, which raises the question: do we need similar large scale annotation efforts to learn generic features for images from each such different modality?

We answer this question in this paper and propose a technique to transfer learned representations from one modality to another. Our technique uses ‘paired’ images from the two modalities and utilizes the mid-level representations from the labeled modality to supervise learning representations on the paired un-labeled modality. We call our scheme ***supervision transfer*** and show that it is able to successfully transfer supervision across modalities. We also show that our technique leads to learning rich semantic concepts in the unlabeled modality, and that for complementary modalities, the intermediate representations are also complementary.

As a motivating example, consider the case of depth images. While the largest labeled RGB dataset ImageNet [6] consists of over a million labeled images, the size of most existing labeled depth datasets is of the order of a few thousands [33, 36, 22]. At the same time there are a large number of unlabeled RGB and depth image pairs. Our technique leverages this large set of unlabeled paired

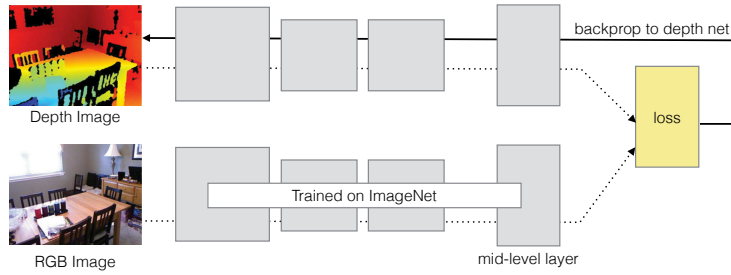


Figure 1: Architecture for supervision transfer: We train a CNN model for a new image modality (like depth images), by teaching the network to reproduce the mid-level semantic representations learned from a well labeled image modality (such as RGB images) for modalities for which there are paired images.

images to transfer the ImageNet supervision on RGB images to depth images. Our technique is illustrated in Figure 1. We use a convolutional neural network that has been trained on labeled images in the ImageNet dataset [6], and use the mid-level representation learned by these CNNs as a supervisory signal to train a CNN on depth images. Our technique for transferring supervision results in improvements in performance for the end task of object detection on the NYUD2 dataset, where we improve the state-of-the-art from 34.2% to 41.7% when using just the depth image and from 46.2% to 49.1% when using both RGB and depth images together.

Though we show detailed experimental results for supervision transfer from RGB to depth images, our technique is equally applicable to images from other paired modalities. To demonstrate this, we show additional transfer results from RGB images to optical flow images where we improve mean average precision for action detection on the JHMDB dataset [23] from 31.7% to 35.7% when using just the optical flow image and no supervised pre-training.

Our technique is a reminiscent of the distillation idea from Hinton *et al.* [18]. Hinton *et al.* [18] extended the model compression idea from Caruana and colleagues [2] to what they call ‘distillation’ and showed how large models trained on large labeled datasets can be compressed by using the soft outputs from the large model as targets for a much smaller model operating on the same modality. Our work here is a generalization of this idea, and a) allows for transfer of supervision at arbitrary semantic levels, and b) additionally enables transfer of supervision between different modalities.

2 Related Work

There has been a large body of work on transferring knowledge between different visual domains, belonging to the *same* modality. Initial work [26, 14, 1, 8, 20] studied the problem in context of shallow image representations. While [26, 14] sought to learn transformations between well labeled source and sparsely labeled target domains, [1] use the source models as a parameter regularizer for target models, [8, 20] combine these two approaches into a single joint optimization problem. Chopra *et al.* [4] introduced one of the first deep architectures for visual adaptation by replicating feature extraction for each domain and producing intermediate interpolated domains, while Ghifary *et al.* [10] showed a single layer neural net could be used to learn the feature transformation between simple domain shifts.

More recently, with the introduction of supervised CNN models by Krizhevsky *et al.* [25], the community has been moving towards a generic set of features which can be specialized to specific tasks and domains at hand [7, 12, 11, 31, 19] and traditional visual adaptation techniques can be used in conjunction with such features [21]. More recently, unsupervised domain adaptation techniques have been introduced which learn to adapt deep representations so as to minimize the discrepancy between the source and target distributions [39, 9, 29].

All these lines of work study and solve the problem of domain adaptation within the same modality. In contrast, our work here tackles the problem of domain adaptation *across different modalities*. Most methods for intra-modality domain adaptation described above start from an initial set of features on the target domain, and *a priori* it is unclear how this can be done when moving across modalities, limiting the applicability of aforementioned approaches to our problem. This cross-

model transfer problem has received much less attention, most notable among those include the works from Christoudias *et al.* [5] and Ngiam *et al.* [30]. While Christoudias *et al.* hallucinate the modalities during training time, Ngiam *et al.* focus on the problem of jointly embedding multiple modalities in a shared feature space. Our work instead transfers generic knowledge learned from a large set of labeled images of one modality to completely unlabeled images from a new modality.

3 Supervision Transfer

Let us assume we have a modality \mathcal{M}_d with unlabeled data, D_d for which we would like to train a rich representation. We will do so by transferring information from a separate modality, \mathcal{M}_s , which has a large labeled set of images, \mathcal{D}_s , and a corresponding K layered rich representation. We assume this rich representation is layered although our proposed method will work equally well for non-layered representations. We use convolutional neural networks as our layered rich representation.

We denote this image representation as $\Phi = \{\phi_{\mathcal{M}_s, D_s}^i, i \in [1 \dots K]\}$. $\phi_{\mathcal{M}_s, D_s}^i$ is the i^{th} layer representation for modality \mathcal{M}_s which has been trained on labeled images from dataset D_s , and it maps an input image from modality \mathcal{M}_s to a feature vector in \mathbb{R}^{n_i} .

$$\phi_{\mathcal{M}_s, D_s}^i : \mathcal{M}_s \mapsto \mathbb{R}^{n_i} \quad (1)$$

Feature vectors from consecutive layers in such layered representations are related to one another by simple operations like non-linearities, convolutions, pooling, normalizations and dot products (for example layer 2 features may be related to layer 1 features using a simple non-linearity like max with 0: $\phi_{\mathcal{M}_s, D_s}^2(x) = \max(0, \phi_{\mathcal{M}_s, D_s}^1(x))$). Some of these operations like convolutions and dot products have free parameters. We denote such parameters associated with operation at layer i by w_s^i . The structure of such architectures (the sequence of operations, and the size of representations at each layer, *etc.*) is hand designed or validated using performance on an end task. Such validation can be done on a small set of annotated images. Estimating the model parameters w_s^i is much more difficult. The number of these parameters for most reasonable image models can easily go up to a few millions. Heretofore, state-of-the-art models require discriminative learning of these parameters using a large labeled training set.

Now suppose we want to learn a rich representation for images from modality \mathcal{M}_d , for which we do not have access to a large dataset of labeled images. We assume we have already hand designed an appropriate architecture $\Psi = \{\psi_{\mathcal{M}_d}^i, \forall i \in [1 \dots L]\}$. The task then is to effectively learn the parameters associated with various operations in the architecture, without having access to a large set of annotated images for modality \mathcal{M}_d . As before, we denote these parameters to be learned by $W_d^{[1 \dots L]} = \{w_d^i, \forall i \in [1 \dots L]\}$

In addition to D_s , let us assume that we have access to a large dataset of *un-annotated paired* images from modalities \mathcal{M}_s and \mathcal{M}_d . We denote this dataset by $U_{s,d}$. By paired images we mean a set of images of the same scene in two different modalities. Our proposed scheme for training rich representations for images of modality \mathcal{M}_d is to learn the representation Ψ such that the image representation $\psi_{\mathcal{D}}^L(I_d)$ for image I_d matches the image representation $\phi_{\mathcal{M}_s, D_s}^{i^*}(I_s)$ for its image pair I_s in modality \mathcal{M}_s for some chosen and fixed layer $i^* \in [1 \dots K]$. We measure the similarity between the representations using an appropriate loss function f (for example, euclidean loss). Note that the representations $\psi_{\mathcal{M}_s}^{i^*}$ and $\phi_{\mathcal{M}_d}^L$ may not have the same dimensions. In such cases we embed features $\psi_{\mathcal{M}_d}^L$ into a space with the same dimension as $\phi_{\mathcal{M}_s}^{i^*}$ using an appropriate simple transformation function t (for example a linear or affine function).

$$\min_{W_d^{[1 \dots L]}} \sum_{(I_s, I_d) \in U_{s,d}} f\left(t\left(\psi_{\mathcal{M}_d}^L(I_d)\right), \phi_{\mathcal{M}_s, D_s}^{i^*}(I_s)\right) \quad (2)$$

We call this process *supervision transfer* from layer i^* in Φ of modality \mathcal{M}_s to layer L in Ψ of modality \mathcal{M}_d .

The recent distillation method from Hinton *et al.* [18] is a specific instantiation of this general method, where a) the two modalities \mathcal{M}_s and \mathcal{M}_d are the same, and b) the *supervision transfer* happens at the very last prediction layer, instead of an arbitrary internal layer in representation Φ .

Our experiments in Section 4 demonstrate that this proposed method for transfer of supervision is a) effective at learning good representations, b) results in transfer of semantic information, and c) the resulting representation can be complementary to the representation in the source modality \mathcal{M}_s if the modalities permit.

4 Experiments

In this section we present experimental results for the NYUD2 dataset where we use color and depth images as the paired modalities, and on the JHMDB video dataset for which we use the RGB and optical flow frames as the two modalities.

Our general experimental framework consists of two steps. The first step is *supervision transfer* as proposed in Section 3, and the second step is to assess the quality of the transferred representation by using it for a downstream task. For both of the datasets we study, we consider the domain of RGB images as \mathcal{M}_s for which there is a large dataset of labeled images D_s in the form of ImageNet [6], and treat depth and optical flow respectively as \mathcal{M}_d . These choices for \mathcal{M}_s and \mathcal{M}_d are of particular practical significance, given the lack of large labeled datasets for depth images and optical flow, at the same time, the abundant availability of paired images coming from RGB-D sensors (for example Microsoft Kinect) and videos on the Internet respectively.

For our layered image representation models, we use convolutional neural networks (CNNs) [27, 25]. These networks have been shown to be very effective for a variety of image understanding tasks [7]. We experiment with the network architectures from Krizhevsky *et al.* [25] (denoted AlexNet), Simonyan and Zisserman [35] (denoted VGG) and Chatfield *et al.* [3], and use the models pre-trained on ImageNet [6] from the Caffe [24] Model Zoo.

We use an architecture similar to [25] for the layered representations for depth and flow images. We do this in order to be able to compare to past works which learn features on depth and flow images [16, 13]. Validating different CNN architectures for depth and flow images is a worthwhile scientific endeavor, which has not been undertaken so far, primarily because of lack of large scale labeled datasets for these modalities. Our work here provides a method to circumvent the need for a large labeled dataset for these and other image modalities, and will naturally enable exploring this question in the future, however we do not delve in this question in the current work.

We next describe our design choices for which layers to transfer supervision between, and the specification of the loss function f and the transformation function t . In all the experiments we report in this paper, we transfer supervision from `pool5` layer of one network to another. Experiments in [12] show that the representation at `pool5` layers are fairly semantic and may also correspond to object parts. Intuitively, the considerations while picking what layer pair to use for transfer are as follows. First, the source layers i^* that we are transferring from should capture mid-level or high-level semantics rather than low-level image statistics. Low-level image statistics are bound to differ between different modalities and it is unreasonable to expect that they will transfer well (for example, filters in `conv1` layers in [25] respond to color which is as such absent in depth images). Second, the layers should be at comparable semantic level, transferring supervision from `pool5` to `conv1` is going to lead to a very hard learning problem. Finally, one would expect it is best to transfer from essentially the layer closest to the labels to enable as much *supervision transfer* as possible, though in our initial experiments we found transfer to work better from an intermediate layer as compared to the final layers. We choose `pool5` as it also has the advantage that it can be computed in a fully convolutional manner on the whole image at once, resulting in large amounts of shared computation, speeding up the transfer process.

For the function f , we use $L2$ distance between the feature vectors, $f(\mathbf{x}, \mathbf{y}) = \|\mathbf{x} - \mathbf{y}\|_2^2$. We also tried $f(\mathbf{x}, \mathbf{y}) = \mathbf{1}(\mathbf{y} > \tau) \cdot \log p(\mathbf{x}) + \mathbf{1}(\mathbf{y} \leq \tau) \cdot \log(1 - p(\mathbf{x}))$ (where $p(x) = \frac{e^{\alpha x}}{1+e^{\alpha x}}$, $\mathbf{1}(x)$ is the indicator function), for some reasonable choices of α and τ but that resulted in worse performance in initial experiments and we did not experiment with it further.

Finally, the choice of the function t varies with different pairs of networks. As noted above, we train using a fully convolutional architecture. This requires the spatial resolution of the two layers i^* in Φ and L in Ψ to be similar, which is trivially true if the architectures Φ and Ψ are the same. When they are not (for example when we transfer from VGG net to AlexNet), we adjust the padding in the AlexNet to obtain the same spatial resolution at `pool5` layer.

This apart, we introduce an adaptation layer comprising of 1×1 convolutions followed by *ReLU* to map from the representation at layer L in Ψ to layer i^* in Φ . This accounts for difference in the number of neurons (for example when adapting from VGG to AlexNet), or even when the number of neurons are the same, allows for domain specific fitting. For VGG to AlexNet transfer we also needed to introduce a scaling layer to make the average norm of features comparable between the two networks.

4.1 Transfer to Depth Images

We first demonstrate how we transfer supervision from color images to depth images as obtained from a range sensor like the Microsoft Kinect. As described above, we do this set of experiments on the NYUD2 dataset [32] and show results on the task of object detection [16]. The NYUD2 dataset consists of 1449 paired RGB and D images. These images come from 464 different scenes and were hand selected from the full video sequence while ensuring ensure diverse scene content [32]. The full video sequence that comes with the dataset has over 400K RGB-D frames.

In all our experiments we report numbers on the standard *val* and *test* splits that come with the dataset [32, 16]. Images in these splits have been selected while ensuring that all frames belonging to the same scene are contained entirely in exactly one split.

The downstream task that we study here is that of object detection. We follow the experimental setup from Gupta *et al.* [16] for object detection and study the 19 category object detection problem, and use mean average precision (mAP) to measure performance.

Baseline Detection Model We use the model from Gupta *et al.* [16] for object detection. Their method builds off R-CNN [12]. In our initial experiments we adapted their model to the more recent Fast R-CNN framework [11]. We summarize our key findings here. First, [16] trained the final detector on both RGB and D features jointly. We found training independent models all the way and then simply averaging the class scores before the SoftMax performed better. While this is counter-intuitive, we feel it is plausible given limited amount of training data. Second, [16] use features from the `fc6` layer and observed worse performance when using `fc7` representation; in our framework where we are training completely independent detectors for the two modalities, using `fc7` representation is better than using `fc6` representation. Finally, using bounding box regression boosts performance. Here we simply average the predicted regression target from the detectors on the two modalities. All this analysis helped us boost the mean AP^b on the *test* set from 38.80% as reported by [16, 15] to 44.39%, using the same CNN network and supervision. This already is the state-of-the-art result on this dataset and we use this as a baseline for the rest of our experiments. We denote this model as ‘[16] + Fast R-CNN’. We followed the default setup for training Fast R-CNN, 40K iterations, base learning rate of 0.001 and stepping it down by a factor of 10 after every 30K iterations, except that we finetune all the layers, and use 688px length for the shorter image side.

Note that Gupta *et al.* [16] embed depth images into a geocentric embedding which they call HHA (HHA encodes horizontal disparity, height above ground and angle with gravity) and use the AlexNet architecture to learn HHA features and *copy over the weights from the RGB CNN that was trained for 1000 way classification [25] on ImageNet [6]* to initialize this network. All through this paper, we stick with using HHA embedding¹ to represent the input depth images, and their network architecture, and show how our proposed *supervision transfer* scheme improves performances over their technique for initialization. We summarize our various transfer experiments below:

Does supervision transfer work? The first question we investigate is if we are able to transfer supervision to a new modality. To understand this we conducted the following three experiments:

1. **no init**: randomly initialize the depth network using weight distributions typically used for training on ImageNet and simply train this network for the final task. While training this network we train for 100K iterations, start with a learning rate on 0.01 and step it down by a factor of 10 every 30K iterations.
2. **copy from RGB**: copy weights from a RGB network that was trained on ImageNet. This is same as the scheme proposed in [16]. This network is then trained using the standard Fast R-CNN settings.

¹We use the term depth and HHA interchangeably.

Does supervision transfer work?	Is this transfer of supervision semantic?	Are the representations complementary?
no init	22.7	copy from RGB (ft f_c only) 19.8
copy from RGB	25.1	supervision transfer adapted (ft f_c only) AlexNet* \rightarrow AlexNet 30.0
supervision transfer AlexNet \rightarrow AlexNet	29.7	supervision transfer adapted (ft f_c only) VGG* \rightarrow AlexNet 32.2
supervision transfer adapted AlexNet* \rightarrow AlexNet	30.5	supervision transfer adapted VGG* \rightarrow AlexNet 33.6
		[RGB]: RGB network on RGB images AlexNet 22.3
		[RGB] + copy from RGB 33.8
		[RGB] + supervision transfer adapted AlexNet* \rightarrow AlexNet 35.6
		[RGB] + supervision transfer adapted VGG* \rightarrow AlexNet 37.0

Table 1: We evaluate different aspects of our *supervision transfer* scheme on the object detection task on the NYUD2 *val* set using the mAP metric. Left column demonstrates that our scheme for pre-training is better than alternatives like no pre-training, and copying over weights from RGB networks. The middle column demonstrates that our technique leads to transfer of mid-level semantic features which by themselves are highly discriminative, and that improving the quality of the supervisory network translated to improvements in the learned features. Finally, the right column demonstrates that the learned features on the depth images are still complementary to the features on the RGB image they were supervised with.

3. ***supervision transfer*:** train layers `conv1` through `pool5` from random initialization using the *supervision transfer* scheme as proposed in Section 3, on the paired RGB and D images from the video sequence from NYUD2 for scenes contained in the training set. We sampled a frame every 0.5 to 1 second. We then plug in these trained layers for training in Fast R-CNN and initialize the f_c6 , f_c7 and classifier layers randomly.

We report the results in Table 1. We see that ‘copy from RGB’ surprisingly does better than ‘no init’, which is consistent with what Gupta *et al.* report in [16], but our scheme for *supervision transfer* outperforms both these baselines by a large margin from 25.1% to 29.7% on average. We also experimented with using a RGB network Ψ that has been adapted for object detection on this dataset for supervising the transfer and found that this boosted performance further from 29.7% to 30.5% (denoted ‘supervision transfer adapted’ in Table 1, AlexNet* indicates RGB AlexNet that has been adapted for detection on the dataset). We use this scheme for all subsequent experiments. We visualize the filters from the first layer for these different schemes of transfer in Figure 2, and observe that our training scheme learns reasonable filters and find that these filters are of different nature than filters learned on RGB images.

Is this transfer of supervision semantic? The next question we ask is if our *supervision transfer* scheme actually transfers semantic information or does it only end up setting up the initial layers in the right ballpark. To answer this question, we conducted the following two experiments.

1. **Quality of transferred `pool5` representation:** The first experiment was to evaluate the quality of the transferred `pool5` representation. To do this, we froze the network parameters for layers `conv1` through `pool5` to be those learned during the transfer process, and only learn parameters in f_c6 , f_c7 and classifier layers during Fast R-CNN training (denoted ‘supervision transfer adapted (ft f_c only)'). We see that there is only a moderate degradation in performance for our learned features from 30.5% to 30.0% indicating that the features learned on depth images at `pool5` are semantically informative, and that we are able to transfer more than just structure in the lower layers of the network.
2. **Improved transfer using better supervising network Φ :** The second experiment investigated if performance improves as we improve the quality of the supervising network. To do this, we transferred supervision from VGG net instead of AlexNet². VGG net has been shown to be better than AlexNet for a variety of vision tasks (for example object detection [12] (see arXiv v5)). As before we report performance when freezing parameters till `pool5`, and learning all the way. We see that using a better supervising net results in learning better features for depth images: when the representation is frozen till `pool5` we see performance improves from 30.0% to 32.2%, and when we finetune all the layers performance goes up to 33.6% as compared to 30.5% for AlexNet.

²To transfer from VGG to AlexNet, we use 150K transfer iterations instead of 100K. Running longer helps for VGG to AlexNet transfer by 1.5% and much less (about 0.5%) for AlexNet to AlexNet transfer.

method	modality	RGB Arch.	D Arch.	bath tub	bed	book shelf	box	chair	counter	desk	door	dresser	garbage bin	lamp	monitor	night stand	pillow	sink	sofa	table	tele vision	toilet	mean
Fast R-CNN [11]	RGB	AlexNet	-	7.9	51.2	37.0	1.5	31.3	35.4	9.4	22.4	28.9	19.3	31.0	35.9	24.1	26.4	24.6	39.7	16.6	32.9	53.5	27.8
Fast R-CNN [11]	RGB	VGG	-	37.4	69.1	47.0	2.9	44.4	48.6	11.5	28.7	43.1	33.6	32.9	50.9	32.6	34.4	39.0	50.3	24.5	44.1	61.5	38.8
Gupta <i>et al.</i> [16]	RGB + D	AlexNet	AlexNet	36.4	70.8	35.1	3.6	47.3	46.8	14.9	23.3	38.6	43.9	37.6	52.7	40.7	42.4	43.5	51.6	22.0	38.0	47.7	38.8
Gupta <i>et al.</i> [15]	RGB + D	AlexNet	AlexNet	39.4	73.6	38.4	5.9	50.1	47.3	14.6	24.4	42.9	51.5	36.2	52.1	41.5	42.9	42.6	54.6	25.4	48.6	50.2	41.2
Gupta <i>et al.</i> [16] + Fast R-CNN	RGB + D	AlexNet	AlexNet	37.1	78.3	48.5	3.3	45.3	54.6	21.9	28.5	48.6	41.9	36.2	49.2	43.7	40.2	62.1	29.2	44.3	63.6	44.4	
Our (<i>supervision transfer</i>)	RGB + D	AlexNet	AlexNet	45.6	78.7	48.5	4.3	50.5	57.8	21.4	29.6	54.0	41.6	45.4	61.2	57.9	47.3	48.9	63.2	29.5	50.0	60.1	47.1
Gupta <i>et al.</i> [16] + Fast R-CNN	RGB + D	VGG	AlexNet	47.2	80.4	52.8	4.2	49.7	53.0	22.4	33.7	52.1	44.4	39.2	64.6	47.5	45.1	42.1	63.2	31.4	42.1	63.0	46.2
Our (<i>supervision transfer</i>)	RGB + D	VGG	AlexNet	50.6	81.0	52.6	5.4	53.0	56.1	20.9	34.6	57.9	46.2	42.5	62.9	54.7	49.1	50.0	65.9	31.9	50.1	68.0	49.1
Gupta <i>et al.</i> [16] + Fast R-CNN	D	-	AlexNet	28.8	79.1	30.3	1.5	42.6	42.7	17.2	13.4	31.6	23.7	29.9	40.2	36.2	40.5	23.4	59.9	26.4	24.9	58.3	34.2
Our (<i>supervision transfer</i>)	D	-	AlexNet	31.2	80.7	38.6	2.5	52.2	52.2	17.2	18.2	50.8	35.1	37.4	51.3	50.5	43.4	41.0	63.5	29.3	37.4	59.8	41.7

Table 2: Object Detection AP(%) on NYUD2 test set: We compare our performance against several state-of-the-art methods. RGB Arch. and D Arch. refers to the CNN architecture used by the detector. We see when using just the depth image, our method is able to improve performance from 34.2% to 41.7%. When used in addition to features from the RGB image, our learned features improve performance from 44.4% to 47.1% (when using AlexNet RGB features) and from 46.2% to 49.1% (when using VGG RGB features) over past methods for learning features from depth images.

method	modality	brush hair	catch	clap	climb stairs	golf	jump	kick ball	pick	pour	pullup	push	run	shoot ball	shoot bow	shoot gun	sit	stand	swing baseball	throw	walk	wave	mean
Gkioxari <i>et al.</i> [13]	RGB	55.8	25.5	25.1	24.0	77.5	1.9	5.3	21.4	68.6	71.0	15.4	6.3	4.6	41.1	28.0	9.4	8.2	19.9	17.8	29.2	11.5	27.0
Gkioxari <i>et al.</i> [13]+Fast R-CNN	RGB	47.2	35.2	30.1	23.9	84.4	2.2	10.6	20.7	79.7	78.7	25.2	14.4	8.7	45.3	34.2	11.7	13.3	39.0	19.1	23.9	23.9	32.0
Gkioxari <i>et al.</i> [13]	flow	32.3	5.0	35.6	30.1	58.0	7.8	2.6	16.4	55.0	72.3	8.5	6.1	3.9	47.8	7.3	24.9	26.3	36.3	4.5	22.1	7.6	24.3
Gkioxari <i>et al.</i> [13]+Fast R-CNN	flow	54.9	17.0	52.5	56.5	81.2	15.0	10.9	28.9	72.7	86.6	20.4	17.5	10.2	61.9	25.5	31.4	42.4	53.8	10.9	38.6	17.3	38.4
no init	flow	44.3	11.0	42.8	38.7	76.1	10.6	6.6	23.1	62.1	84.0	15.4	9.6	6.8	60.0	22.8	29.6	26.8	43.5	10.7	30.8	9.8	31.7
Our (<i>supervision transfer</i>)	flow	54.6	17.7	45.1	54.9	80.3	14.6	9.7	28.2	69.3	84.8	19.9	15.6	7.2	49.6	29.4	29.5	28.4	49.5	11.6	36.3	13.0	35.7

Table 3: Action Detection AP(%) on the JHMDB test set: We report action detection performance on the test set of JHMDB using RGB or flow images. Bottom part of the table, compares our method *supervision transfer* against the baseline of random initialization, and the ceiling using fully supervised pre-training method from [13]. Our method reaches more than half the way towards fully supervised pre-training.

Is the learned representation complementary to the representation on the source modality? The next question we ask is if the representation learned on the depth images complementary to the representation on the RGB images from which it was learned. To answer this question we look at the performance when using both the modalities together. We do this the same way that we describe for the baseline model and simply average the category scores and regression targets from the RGB and D detectors. Table 1(right) reports our findings. Just using RGB images gives us a performance of 22.3%. Combining this with the HHA network as initialized using the scheme from Gupta *et al.* [16] boosts performance to 33.8%. Initializing the HHA network using our proposed supervision transfer scheme when transferring from AlexNet * to AlexNet gives us 35.6% and when transferring from VGG * to AlexNet gives us 37.0%. These results show that the representations are still complementary and using the two together can help the final performance.

Finally, we report the performance of our best performing supervision transfer scheme (VGG * → AlexNet) on the test set in Table 2. When used with AlexNet for obtaining color features, we obtain a final performance of 47.1% which is about 2.7% higher than the current state-of-the-art on this task (Gupta *et al.* [16] Fast R-CNN). We see similar improvements when using VGG for obtaining color features (46.2% to 49.1%). The improvement when using just the depth image is much larger, 41.7% for our final model as compared to 34.2% for the baseline model which amounts to a 22% relative improvement. Note that in obtaining these performance improvements we are using exactly the same CNN architecture and amount of labeled data.

4.2 Transfer to Flow Images

We now report our experiments for transferring supervision to optical flow images. We consider the end task of action detection on the JHMDB dataset. The task is to detect people doing actions like catch, clap, pick, run, sit in frames of a video. Performance is measured in terms of mean

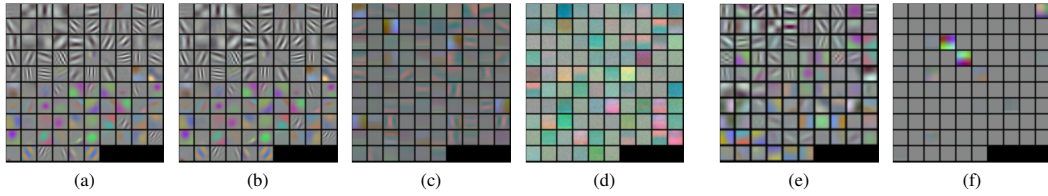


Figure 2: Visualization of learned filters: (a) visualizes filters learned on RGB images from ImageNet data by AlexNet. (b) shows these filters after the finetuning on HHA images, and hardly anything changes visually. (c) shows HHA image filters from our pre-training scheme, which are much different from ones that are learned on RGB images. (d) shows HHA image filters learned without any pre-training. (e) shows optical flow filters learned by [13]. Note that they initialize these filters from RGB filters and these also do not change much over their initial RGB filters. (f) shows filters we learn on optical flow images, which are again very different from filters learned on RGB or HHA images (best viewed in color).

average precision as in the standard PASCAL VOC object detection task and what we used for the NYUD2 experiments in Section 4.1.

A popular technique for getting better performance at such tasks on video data is to additionally use features computed on the optical flow between the current frame and the next frame [34, 13], and we use our *supervision transfer* scheme to learn features for optical flow images in this context.

Detection model For JHMDB we use the experimental setup from Gkioxari and Malik [13] and study the 21 class task. Here again, Gkioxari and Malik build off of R-CNN and we first adapt their system to use Fast R-CNN, and observe similar boosts in performance as for NYUD2 when going from R-CNN to Fast R-CNN framework (Table 3). We denote this model as ‘Gkioxari *et al.* [13]+Fast R-CNN’. We attribute this large difference in performance to a) bounding box regression and b) number of iterations used for training.

Supervision transfer performance We use the videos from UCF 101 dataset [37] for our pre-training. Note that we do not use any labels provided with the UCF 101 dataset, and simply use the videos as a source of paired RGB and flow images. We take 5 frames from each of the $9K$ videos in the *train1* set. We report performance on JHMDB *test* set in Table 3. Note that JHMDB has 3 splits and as in past work, we report the AP averaged across these 3 splits.

We report performance for three different schemes for initializing the flow model: a) **no init** when the flow network is initialized randomly using the weight initialization scheme used for training a RGB model on ImageNet, b) **supervised pre-training** on UCF 101 starting from RGB weights as done by Gkioxari and Malik [13] (denoted by ‘Gkioxari *et al.* [13] + Fast R-CNN’, and c) **supervision transfer** from an RGB model to train optical flow model as per our proposed method. We see that our scheme for *supervision transfer* improves performance from 31.7% achieved when using random initialization to 35.7%, which is more than half way towards what fully supervised pre-training can achieve (38.4%), thereby illustrating the efficacy of our adaptation scheme.

Conclusion In this paper, we have presented an algorithm for transfer of learned representations from a well labeled modality to new unlabeled modalities using unlabeled paired images from the two modalities. This enables us to learn rich representations on unlabeled modalities and obtain large boosts in performance. We believe the advances presented in this paper will allow us to effectively use new modalities for obtaining better performance on standard vision tasks.

Acknowledgments: The authors would like to thank Georgia Gkioxari for sharing her wisdom and experimental setup for the UCF 101 and JHMDB datasets. This work was supported by ONR SMARTS MURI N00014-09-1-1051, a Berkeley Graduate Fellowship, and a NSF Graduate Research Fellowship. We gratefully acknowledge NVIDIA corporation for the donation of Tesla and Titan GPUs used for this research.

References

- [1] Y. Aytar and A. Zisserman. Tabula rasa: Model transfer for object category detection. In *ICCV*, 2011.
- [2] C. Bucilua, R. Caruana, and A. Niculescu-Mizil. Model compression. In *ACM SIGKDD*, 2006.

- [3] K. Chatfield, K. Simonyan, A. Vedaldi, and A. Zisserman. Return of the devil in the details: Delving deep into convolutional nets. In *BMVC*, 2014.
- [4] S. Chopra, S. Balakrishnan, and R. Gopalan. DLID: Deep learning for domain adaptation by interpolating between domains. In *ICML Workshop on Challenges in Representation Learning*, 2013.
- [5] C. M. Christoudias, R. Urtasun, M. Salzmann, and T. Darrell. Learning to recognize objects from unseen modalities. In *Computer Vision–ECCV 2010*, pages 677–691. Springer, 2010.
- [6] J. Deng, W. Dong, R. Socher, L.-J. Li, K. Li, and L. Fei-Fei. ImageNet: A large-scale hierarchical image database. In *CVPR*, 2009.
- [7] J. Donahue, Y. Jia, O. Vinyals, J. Hoffman, N. Zhang, E. Tzeng, and T. Darrell. Decaf: A deep convolutional activation feature for generic visual recognition. In *ICML*, 2014.
- [8] L. Duan, D. Xu, and I. W. Tsang. Learning with augmented features for heterogeneous domain adaptation. In *ICML*, 2012.
- [9] Y. Ganin and V. Lempitsky. Unsupervised Domain Adaptation by Backpropagation. *ArXiv e-prints*, Sept. 2014.
- [10] M. Ghifary, W. B. Kleijn, and M. Zhang. Domain adaptive neural networks for object recognition. *CoRR*, abs/1409.6041, 2014.
- [11] R. Girshick. Fast R-CNN. *arXiv preprint arXiv:1504.08083*, 2015.
- [12] R. Girshick, J. Donahue, T. Darrell, and J. Malik. Rich feature hierarchies for accurate object detection and semantic segmentation. In *CVPR*, 2014.
- [13] G. Gkioxari and J. Malik. Finding action tubes. In *CVPR*, 2015.
- [14] B. Gong, Y. Shi, F. Sha, and K. Grauman. Geodesic flow kernel for unsupervised domain adaptation. In *CVPR*, 2012.
- [15] S. Gupta, P. Arbeláez, R. Girshick, and J. Malik. Aligning 3D models to RGB-D images of cluttered scenes. In *CVPR*, 2015.
- [16] S. Gupta, R. Girshick, P. Arbeláez, and J. Malik. Learning rich features from RGB-D images for object detection and segmentation. In *ECCV*, 2014.
- [17] B. Hariharan, P. Arbeláez, R. Girshick, and J. Malik. Simultaneous detection and segmentation. In *ECCV*, 2014.
- [18] G. E. Hinton, O. Vinyals, and J. Dean. Distilling the knowledge in a neural network. In *NIPS 2014 Deep Learning Workshop*, 2014.
- [19] J. Hoffman, S. Guadarrama, E. Tzeng, R. Hu, J. Donahue, R. Girshick, T. Darrell, and K. Saenko. LSDA: Large scale detection through adaptation. In *NIPS*, 2014.
- [20] J. Hoffman, E. Rodner, J. Donahue, K. Saenko, and T. Darrell. Efficient learning of domain-invariant image representations. In *ICLR*, 2013.
- [21] J. Hoffman, E. Tzeng, J. Donahue, Y. Jia, K. Saenko, and T. Darrell. One-shot learning of supervised deep convolutional models. In *arXiv 1312.6204; presented at ICLR Workshop*, 2014.
- [22] A. Janoch, S. Karayev, Y. Jia, J. T. Barron, M. Fritz, K. Saenko, and T. Darrell. A category-level 3D object dataset: Putting the kinect to work. In *Consumer Depth Cameras for Computer Vision*. 2013.
- [23] H. Jhuang, J. Gall, S. Zuffi, C. Schmid, and M. J. Black. Towards understanding action recognition. In *ICCV*, 2013.
- [24] Y. Jia. Caffe: An open source convolutional architecture for fast feature embedding. <http://caffe.berkeleyvision.org/>, 2013.
- [25] A. Krizhevsky, I. Sutskever, and G. Hinton. ImageNet classification with deep convolutional neural networks. In *NIPS*, 2012.
- [26] B. Kulis, K. Saenko, and T. Darrell. What you saw is not what you get: Domain adaptation using asymmetric kernel transforms. In *CVPR*, 2011.
- [27] Y. LeCun, B. Boser, J. S. Denker, D. Henderson, R. E. Howard, W. Hubbard, and L. D. Jackel. Backpropagation applied to handwritten zip code recognition. *Neural Computation*, 1989.
- [28] J. Long, E. Shelhamer, and T. Darrell. Fully convolutional networks for semantic segmentation. In *CVPR*, 2015.
- [29] M. Long and J. Wang. Learning transferable features with deep adaptation networks. *CoRR*, abs/1502.02791, 2015.
- [30] J. Ngiam, A. Khosla, M. Kim, J. Nam, H. Lee, and A. Y. Ng. Multimodal deep learning. In *Proceedings of the 28th International Conference on Machine Learning (ICML-11)*, pages 689–696, 2011.
- [31] P. Sermanet, D. Eigen, X. Zhang, M. Mathieu, R. Fergus, and Y. LeCun. Overfeat: Integrated recognition, localization and detection using convolutional networks. In *ICLR. CBLS*, April 2014.
- [32] N. Silberman, D. Hoiem, P. Kohli, and R. Fergus. Indoor segmentation and support inference from RGBD images. In *ECCV*, 2012.
- [33] N. Silberman, D. Sontag, and R. Fergus. Instance segmentation of indoor scenes using a coverage loss. In *ECCV*, 2014.
- [34] K. Simonyan and A. Zisserman. Two-stream convolutional networks for action recognition in videos. In *NIPS*, 2014.

- [35] K. Simonyan and A. Zisserman. Very deep convolutional networks for large-scale image recognition. *arXiv preprint arXiv:1409.1556*, 2014.
- [36] S. Song, S. P. Lichtenberg, and J. Xiao. Sun rgb-d: A rgb-d scene understanding benchmark suite. In *CVPR*, 2015.
- [37] K. Soomro, A. R. Zamir, and M. Shah. Ucf101: A dataset of 101 human action classes from videos in the wild. In *CRCV-TR-12-01*, 2012.
- [38] S. Tulsiani and J. Malik. Viewpoints and keypoints. In *CVPR*, 2015.
- [39] E. Tzeng, J. Hoffman, N. Zhang, K. Saenko, and T. Darrell. Deep domain confusion: Maximizing for domain invariance. *CoRR*, abs/1412.3474, 2014.